# Multimodal Brain Tumor Segmentation with Deep Learning

Ian Timmis

*Lawrence Technological University*
*itimmis@ltu.edu*

***Abstract***

*We developed an algorithm for detecting a hierarchy of brain tumor structures in multimodal Magnetic Resonance (MR) Images. A subtask of this algorithm is to output a predicted remaining lifespan for the patient. We propose the use of a U-net-like neural network architecture along with the use of heavy data augmentation to solve this problem. The network was trained on powerful Tesla V100 GPU on the cloud and achieved a 0.584 dice loss on the test set.*

***Keywords:*** *Deep learning, Medical imaging, Image Segmentation, Brain tumor*

## 1. Introduction

All tumors arising from the supportive tissue of the brain are considered Gliomas. Gliomas account for 80 percent of all malignant brain tumors. 16,000 new cases of high-grade gliomas (HGG) are expected to be diagnosed in the United States in 2018. The one-, five- and ten-year survival rates for patients with HGG is 37.2 percent, 5.1 percent, and 2.6 percent respectively. HGG is one of the most lethal cancers. Gliomas are the most common primary brain malignancies. They contain various heterogeneous histological sub-regions, i.e. peritumoral edema, necrotic core, enhancing and non-enhancing tumor core. This heterogeneity of gliomas is also portrayed in their imaging phenotype as their sub-regions are described by varying intensity profiles disseminated across multimodal MRI scans, reflecting varying tumor biological properties. Due to this highly heterogeneous appearance and shape, segmentation of brain tumors in multimodal MRI scans is one of the most challenging tasks in medical image analysis. [3]

## 2. Input Dataset

The dataset described in this paper was released by the Medical Image Computing and Computer Assisted Interventions Conference (MICCAI) 2017 [1]. The dataset includes multi-institutional clinically acquired MR Images of 285 patients with glioblastoma (GBM/HGG) and lower grade glioma (LGG), with pathologically confirmed diagnosis. These multimodal scans describe a) native (T1) and b) post-contrast T1-weighted (T1Gd), c) T2-weighted (T2), and d) T2 Fluid Attenuated Inversion Recovery (FLAIR) volumes and were acquired with different clinical protocols and various scanners from multiple (n=19) institutions. The dataset also includes some metadata on 168 of the patients. This metadata includes the age of the patient and the amount of days left the patient had to live, hereafter referred to as the survival rate. [5,6,7,8]

## 3. Data Exploration

### 3.1. Metadata

In order to get better acquainted with the metadata, a few visualizations have been developed to analyze the patient age and patient survival. In Figure 1, we analyze the Kernel Density Estimation as well as a Histogram of the patient age and patient survival distributions.

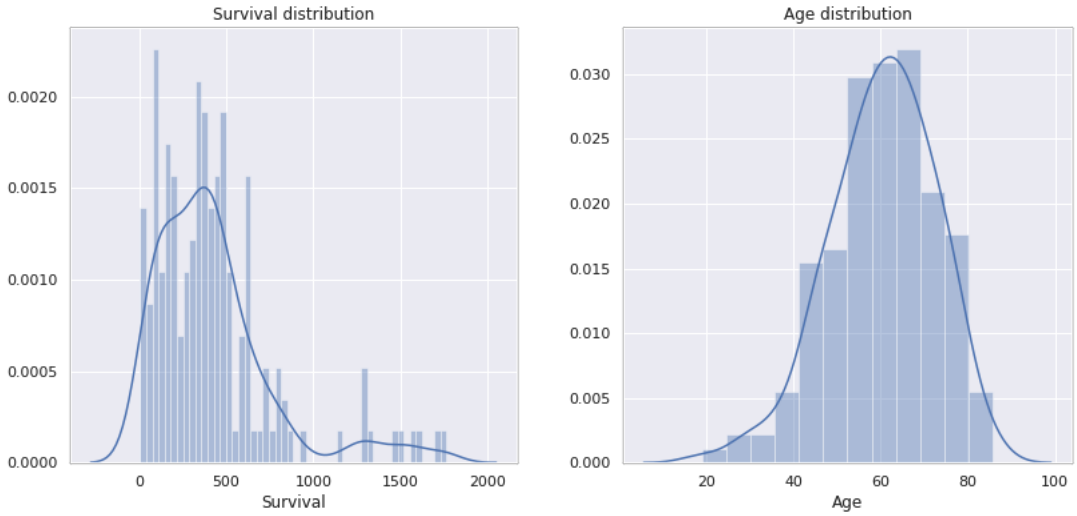


**Figure 1. Patient Age and Patient Survival distributions**

In Figure 2, we generate a scatterplot with the patient age and patient survival. We demonstrate that there is a -0.3722 correlation between these data points. This negative correlation suggests that higher age indicates lower survival rates.

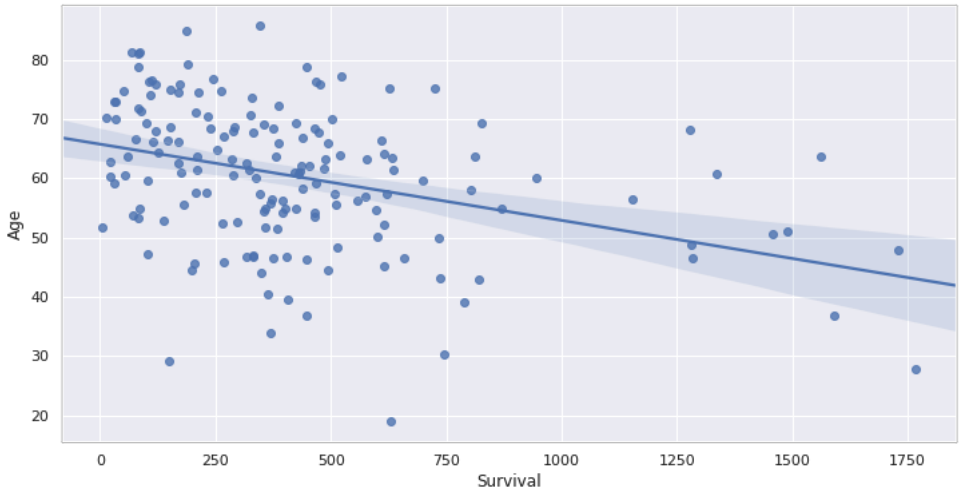


**Figure 2. Patient Age / Patient Survival Regression Plot**

Although, as we can see in Figure 3, if we generate a Kernel Density Estimation to observe the bivariate distribution of the patient age and patient survival, we notice that most of our data consists of patients that are higher in age and lower in survival rate. This indicates that our correlation noted earlier may be invalid. To develop a model to estimate the survival rate on new patients we will have to incorporate MRI data in the prediction.

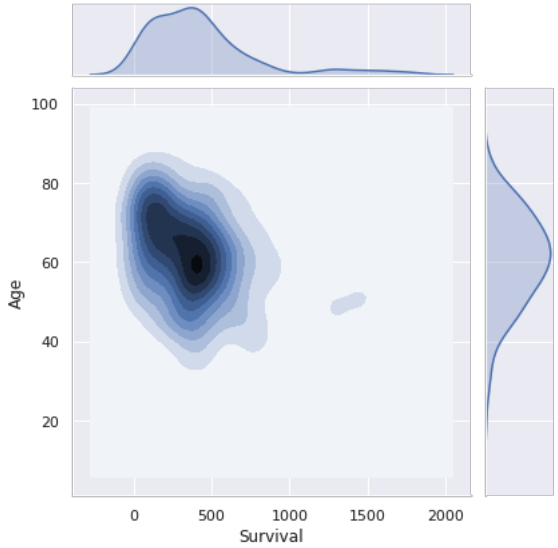


**Figure 3. Patient Age and Survival Kernel Density Estimation**

### 3.2. Magnetic Resonance Images

Each training example contains MR images of 4 different modalities and a labeled segmentation mask. The modalities include T1, T1ce, T2, and FLAIR. An example of this can be seen in Figure 4.

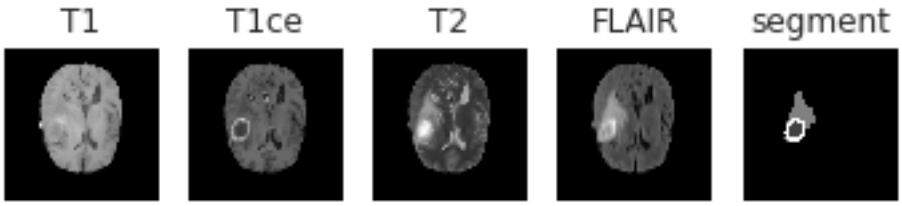


**Figure 4. Example of MR Images and Segmentation Map**

## 4. Method

### 4.1. Preprocessing

We standardize the pixel values by calculating the z-score. The standardization can be described as follows:

$$Z = \frac{X - \mu}{\sigma}$$

To make up for the small dataset, we augment the data 9 times for every training example. This increased the training set by an order of magnitude. We augment the data by performing random flipping on the vertical axis, elastic transformations, rotations, shifting, shearing and zooming. An example of this can be seen in figure 5.

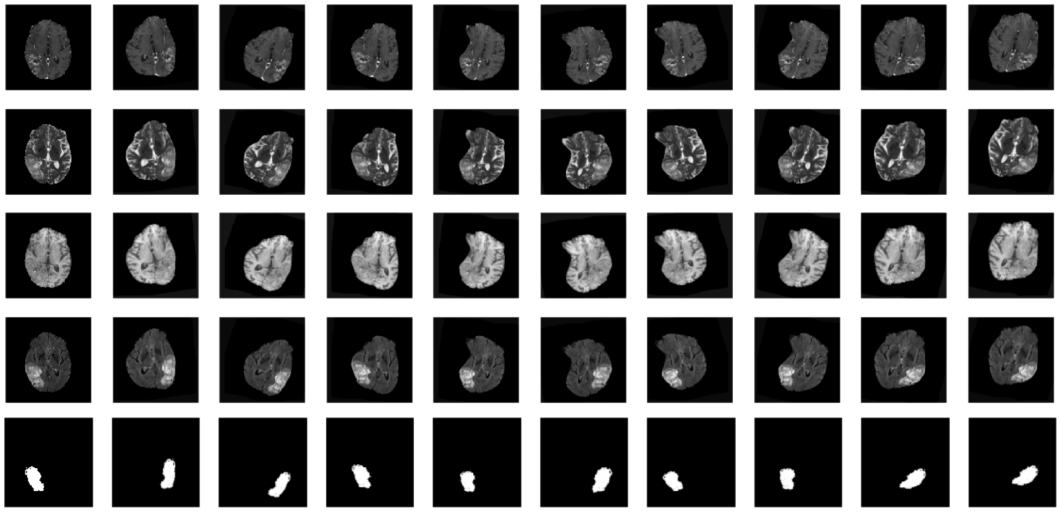

**Figure 5. Augmentation Example**

### 4.3. Problem Formulation

The task of brain tumor segmentation is an image segmentation problem. We use the Jaccard Dice Coefficient to calculate the loss in the network. The Jaccard Dice Coefficient can be described as follows:

$$dice = \frac{2TP}{2TP + FP + FN}$$

where TP, FP and FN represent true positive, false positive and false negative respectively.

### 4.4. Neural Network Architecture

We propose the use of a U-Net-like architecture (see Figure 5) to segment the brain tumors from the MR Images [2]. This network uses an encoder-decoder architecture. The encoder uses convolution operations to learn a latent representation which is then fed into the decoder. The decoder runs convolution-transpose operations to transform the latent representation into a predicted segmentation map.

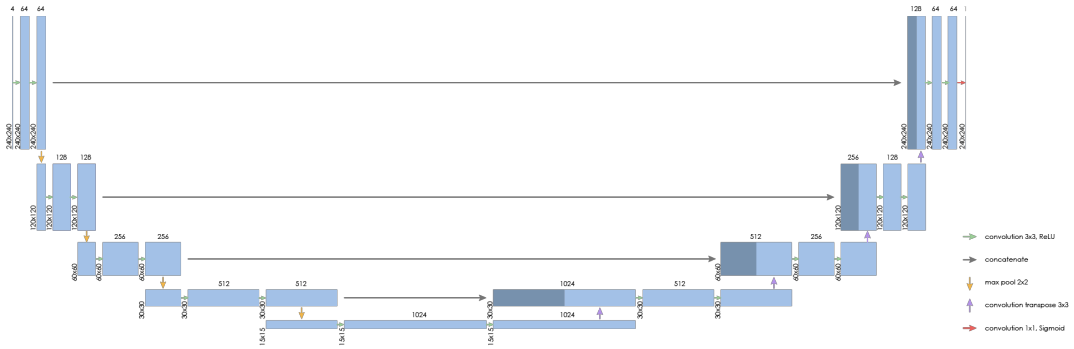


**Figure 6. Model Architecture**

### 4.5. Training

We train the network for 12 hours (1 training epoch) on a Tesla V100 GPU. We trained two models simultaneously using the Adam optimization method [4]. One model was trained with the standard learning rate of 0.001 and the other was trained with a non-standard learning rate of 0.0001. We used a mini-batch size of 32 for both models.

We split the data with a 50-25-25 Train-Validation-Test split (before augmentation). This results in a training set size of 22,010 (220,100 with augmentation), a validation set of 10,540, and a test set of 10,540. Augmentation was only performed on training data, not on validation or testing data. HGG and LGG examples were both evenly split amongst the datasets.

The model trained with the standard Adam learning rate achieved a training loss of 0.442 and validation loss of 0.641 indicating slight overfitting to the training set. The model with the non-standard Adam learning rate achieved a training loss of 0.611 and a validation loss of 0.58. The non-standard rate appears to generalize better to unseen data, so the evaluation will be on that model.

## 5. Results

The model achieved a 0.5842 which indicates ~41% intersection over union.

## 6. Acknowledgments

We would like to acknowledge Dr. CJ Chung for the support in paying for the cloud computing resources required for the development of this model to take place.

**References**

1. Menze, B. H., Jakab, A., Bauer, S., Kalpathy-Cramer, J., Farahani, K., Kirby, J., ... & Lanczi, L. (2015). The multimodal brain tumor image segmentation benchmark (BRATS). *IEEE transactions on medical imaging, 34*(10), 1993.
2. Ronneberger, O., Fischer, P., & Brox, T. (2015, October). U-net: Convolutional networks for biomedical image segmentation. In *International Conference on Medical image computing and computer-assisted intervention* (pp. 234-241). Springer, Cham.
3. Tocagen, https://tocagen.com/patients/brain-cancer/brain-cancer-statistics, last accessed 2018/12/21
4. Kingma, D. P., & Ba, J. (2014). Adam: A method for stochastic optimization. arXiv preprint arXiv:1412.6980.
5. Menze BH, Jakab A, Bauer S, Kalpathy-Cramer J, Farahani K, Kirby J, Burren Y, Porz N, Slotboom J, Wiest R, Lanczi L, Gerstner E, Weber MA, Arbel T, Avants BB, Ayache N, Buendia P, Collins DL, Cordier N, Corso JJ, Criminisi A, Das T, Delingette H, Demiralp Γ‡, Durst CR, Dojat M, Doyle S, Festa J, Forbes F, Geremia E, Glocker B, Golland P, Guo X, Hamamci A, Iftekharuddin KM, Jena R, John NM, Konukoglu E, Lashkari D, Mariz JA, Meier R, Pereira S, Precup D, Price SJ, Raviv TR, Reza SM, Ryan M, Sarikaya D, Schwartz L, Shin HC, Shotton J, Silva CA, Sousa N, Subbanna NK, Szekely G, Taylor TJ, Thomas OM, Tustison NJ, Unal G, Vasseur F, Wintermark M, Ye DH, Zhao L, Zhao B, Zikic D, Prastawa M, Reyes M, Van Leemput K. "The Multimodal Brain Tumor Image Segmentation Benchmark (BRATS)", IEEE Transactions on Medical Imaging 34(10), 1993-2024 (2015) DOI: 10.1109/TMI.2014.2377694
6. [2] Bakas S, Akbari H, Sotiras A, Bilello M, Rozycki M, Kirby JS, Freymann JB, Farahani K, Davatzikos C. "Advancing The Cancer Genome Atlas glioma MRI collections with expert segmentation labels and radiomic features", Nature Scientific Data, 4:170117 (2017) DOI: 10.1038/sdata.2017.117
7. [3] Bakas S, Akbari H, Sotiras A, Bilello M, Rozycki M, Kirby J, Freymann J, Farahani K, Davatzikos C. "Segmentation Labels and Radiomic Features for the

Pre-operative Scans of the TCGA-GBM collection", The Cancer Imaging Archive, 2017. DOI: 10.7937/K9/TCIA.2017.KLXWJJ1Q

8. [4] Bakas S, Akbari H, Sotiras A, Bilello M, Rozycki M, Kirby J, Freymann J, Farahani K, Davatzikos C. "Segmentation Labels and Radiomic Features for the Pre-operative Scans of the TCGA-LGG collection", The Cancer Imaging Archive, 2017. DOI: 10.7937/K9/TCIA.2017.GJQ7R0EF